

Comparison of periodontal evaluation by cone-beam computed tomography, and clinical and intraoral radiographic examinations

Wenjian Zhang¹  · Shazia Rajani² · Bing-Yan Wang³

Received: 21 February 2017 / Accepted: 12 July 2017 / Published online: 1 August 2017
© Japanese Society for Oral and Maxillofacial Radiology and Springer Japan KK 2017

Abstract

Objectives Cone-beam computed tomography (CBCT) has been widely used in many fields of dentistry. However, little is known about the accuracy of CBCT for evaluation of periodontal status. The objective of this study was to compare and correlate periodontal assessments among CBCT, clinical attachment loss (CAL) measurement, and periapical (PA)/bitewing (BW) radiography.

Methods Eighty patients (28 males, 52 females; age range, 19–84 years) from the University of Texas School of Dentistry at Houston were evaluated retrospectively. Measurements were taken on the central incisors, canines, and first molars of the right maxilla and left mandible. CAL was extracted from periodontal charts. The radiographic distance from the cementum–enamel junction (CEJ) to the alveolar crest was measured for tooth mesial and distal sites on PA/BW and CBCT images using MiPacs software and Anatomage Invivo software, respectively. One-way ANOVA and Pearson analysis were performed for statistical analyses.

Results The CEJ–crest distances for CBCT, PA/BW, and CAL were 2.56 ± 0.12 , 2.04 ± 0.12 , and 2.08 ± 0.17 mm (mean \pm SD), respectively. CBCT exhibited larger values than the other two methods ($p < 0.05$). There were highly significant positive correlations among CBCT, PA/BW, and CAL measurements at all examined sites ($p < 0.001$). The Pearson correlation coefficient was higher for CBCT with CAL relative to PA/BW with CAL, but the difference was not significant ($r = 0.64$ and $r = 0.55$, respectively, $p > 0.05$).

Conclusions This study validates the suitability of CBCT for periodontal assessment. Further studies are necessary to optimize the measurement methodology with CBCT.

Keywords Cone-beam computed tomography · Clinical attachment loss · Intraoral radiography · Periodontal assessment

Introduction

Periodontitis is a chronic bacterial infection that exhibits gingival inflammation, connective tissue breakdown, alveolar bone destruction, and ultimately tooth loss [1, 2]. Studies have found a high prevalence of periodontitis in the USA, with 46% of adults, representing 64.7 million people, suffering from periodontitis. The prevalence of periodontitis is positively associated with age and negatively associated with socioeconomic and education status of the population [3, 4]. Poor periodontal condition can negatively affect systemic health and contribute to cardiovascular and respiratory diseases as well as pre-term birth [5–7]. Therefore, it is important to diagnose and intervene in this condition at its early stage.

✉ Wenjian Zhang
Wenjian.Zhang@uth.tmc.edu

¹ Department of Diagnostic and Biomedical Sciences, School of Dentistry, University of Texas Health Science Center at Houston, 7500 Cambridge Street, Suite 5366, Houston, TX 77054, USA

² Dental Hygiene Program, School of Dentistry, University of Texas Health Science Center at Houston, 7500 Cambridge Street, Suite 5366, Houston, TX 77054, USA

³ Department of Periodontics and Dental Hygiene, School of Dentistry, University of Texas Health Science Center at Houston, 7500 Cambridge Street, Suite 5366, Houston, TX 77054, USA

Clinically, a periodontal probe remains the primary diagnostic tool to detect the presence and severity of periodontal bone loss [8]. Clinical attachment loss (CAL), one of the important clinical parameters, is measured by the distance from the cementum–enamel junction (CEJ) to the base of the pocket [8]. Although CAL is expected to reflect the level of apical regression of periodontal fiber attachment, it actually records the distance from the CEJ to where the probe tip meets resistance from the tissues. Many factors, such as type and size of probe [9], probing pressure and angulation [10, 11], presence of supragingival or subgingival calculus [12, 13], and inflammatory status [14, 15], can affect the penetration depth of the probe into the periodontal tissue and result in inaccurate readings. Studies have shown that errors may correspond to 30–50% of the final estimated value during periodontal probing [16, 17].

Conventional two-dimensional (2D) intraoral radiographs, including bitewing (BW) and periapical (PA) views, are considered the gold standard radiographic tools for periodontal diagnosis and treatment planning [18]. Generally, a radiographic CEJ–crest distance greater than 1.9 mm indicates periodontal bone loss [19]. These 2D radiographs are easy to acquire and inexpensive, and provide images with high resolution [20, 21]. However, they suffer from the inherent drawback of plain radiographs, namely the provision of a 2D view of three-dimensional (3D) structures. As a consequence, superimposition, distortion, and magnification of the images can compromise the accuracy of periodontal measurements [22–24].

Recently, cone-beam computed tomography (CBCT) has emerged as a promising imaging modality in dentistry. It has established itself as a lower-cost alternative to conventional CT, with high image quality, reduced radiation exposure, and small footprint suitable for most dental offices [25–27]. CBCT generates images with excellent morphologic details and dimensional accuracy, and eliminates the structural distortion and overlapping commonly encountered in 2D imaging [26, 28].

To date, most attention regarding CBCT has been focused on its applications in dental implantology, orthodontics, oral surgery, endodontics, and temporomandibular joint assessment [29–33]. Only about 3% of recent studies in dentistry have evaluated the application of CBCT in periodontics [34]. Based on the limited information in this field, the present study aimed to compare and correlate CBCT periodontal assessment with clinical and 2D intraoral radiographic examinations to define the role of CBCT in periodontal evaluation and treatment planning.

Materials and methods

Subjects

Patients who visited the University of Texas School of Dentistry at the Houston clinic from 2014 were retrospectively screened according to the selection criteria. The inclusion criteria for the subjects were: (1) comprehensive periodontal examination with information entered into the school's electronic health record (EHR); (2) diagnostic-quality full-mouth survey including PA and BW radiographs covering the entire dentition; and (3) diagnostic-quality CBCT scan with coverage of the entire maxilla and mandible. A total of 80 patients were included in the study. The majority of the patients underwent CBCT scans for implant treatment planning. The patients comprised 28 males and 52 females, with an age range of 19–84 years (mean age, 54.9 ± 15.4 years; Table 1). Institutional Review Board (IRB) approval was granted prior to the start of the study (HSC-DB-16-0398). For all subjects, the central incisors, canines, and first molars of the right maxilla and left mandible were assessed according to the methods described below.

Clinical periodontal assessment

All subjects had undergone comprehensive periodontal clinical examinations by pre-doctoral dental students, including measurement of probing depth (PD) and free gingival margin to cementum–enamel junction distance (FGM–CEJ). CAL was calculated automatically based on the formula: $CAL = PD - (FGM - CEJ)$ (Fig. 1).

Intraoral radiographic acquisition and measurements

All intraoral radiographs were taken with a wall-mounted unit (Focus; Instrumentarium Dental, Charlotte, NC, USA)

Table 1 Age and sex distribution of the recruited subjects

Age (years)	Males	Females	Total
<20	1	0	1
20–29	2	3	5
30–39	2	8	10
40–49	4	7	11
50–59	8	9	17
60–69	9	16	25
70–79	2	6	8
≥80	0	3	3
Total	28	52	80

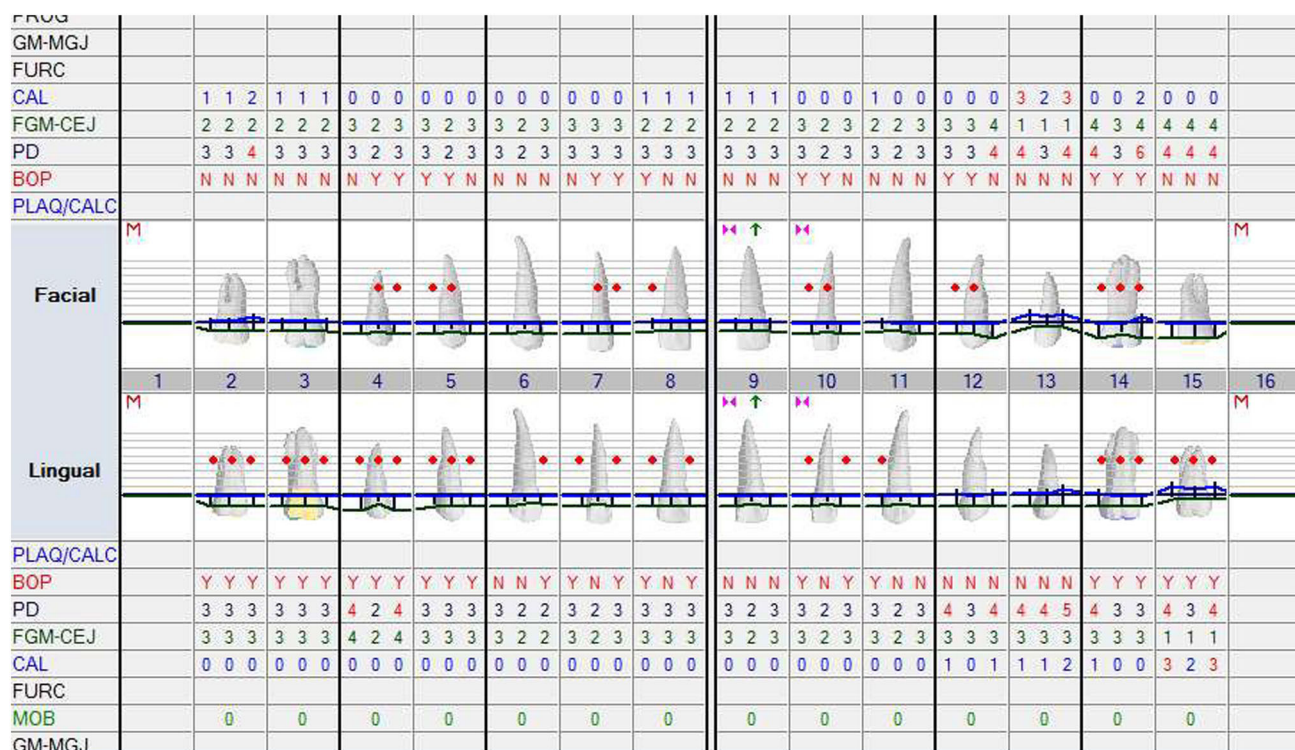


Fig. 1 Periodontal charts extracted from the electronic health record. Clinical attachment loss (CAL) was calculated from the probing depth (PD) and free gingival margin to cementum–enamel junction distance (FGM–CEJ) with the formula: $CAL = PD - (FGM-CEJ)$

operating at 70 kVp and 7 mA. The time settings varied depending on the specific area being targeted. The images were captured with XCP receptor-holding devices (Dentsply Rinn, Elgin, IL, USA) and the paralleling technique on photostimulable phosphor plates (Air Techniques, Melville, NY, USA). The plates were scanned with a Scan-X Intraoral scanner (Air Techniques). The images were imported into the EHR of the School of Dentistry and viewed on a 19-inch flat panel screen (HP Development Company, Palo Alto, CA, USA) with 1920 × 1080 pixel resolution in a dimly lit environment.

For central incisors and canines, CEJ–crest distances were measured on PA radiographs for mesial and distal sites, while for first molars measurements were taken on BW radiographs for both sites (Fig. 2). All of these measurements were made with the linear measurement tool of MiPacs software (Medicor Imaging, Charlotte, NC, USA).

CBCT imaging acquisition and measurements

All CBCT scans covered the maxillary and mandibular arches with a field of view of 150 × 90 mm². The scans were acquired at 90 kVp, 10 mA, 16 s, and 0.2-mm³ voxel size with a Kodak 9500 unit (Carestream Health Inc., Rochester, NY, USA). The CBCT images were reconstructed with Anatomage Invivo 5 software (Anatomage Inc., San Jose, CA, USA) at 1-mm thickness. All CBCT

images were viewed on the same monitor and in the same environment as the intraoral radiographs.

Periodontal assessments were performed on reconstructed cross-sectional and sagittal CBCT views. For cross-sectional view measurement, under the “Arch section” tab, the plane of the cross-sectional cut was determined on the axial and panoramic views. The cut was tangential to the interproximal surface of the tooth and perpendicular to the alveolar ridge on the mesial or distal sites. On the selected cross-sectional view, the CEJ–crest distance was measured on both the buccal and lingual/palatal sides with the linear measurement tool, and the results were averaged (Fig. 3a, b). For teeth where the CEJ was not discernible on cross-sectional views, the nerve tracing tool was used to mark the CEJ. This tool was originally designed to highlight the mandibular canal in red. In the present study, the tool was used to highlight the CEJ instead. More specifically, on the axial view, the slices were screened in an apical-to-coronal direction at the examined tooth. When the enamel layer (more radiopaque than dentin) just showed up, the nerve tracing tool was activated to trace the enamel–dentin junction around the cervical region in red. As shown in Fig. 3c, the CEJ was marked as a cervical red circle on the axial view, which was translated as two red dots (one on the buccal side, and one on the lingual/palatal side) on the cross-sectional view (Fig. 3d). This process made it easier and more reliable to identify the CEJ and obtain periodontal bone level measurements.

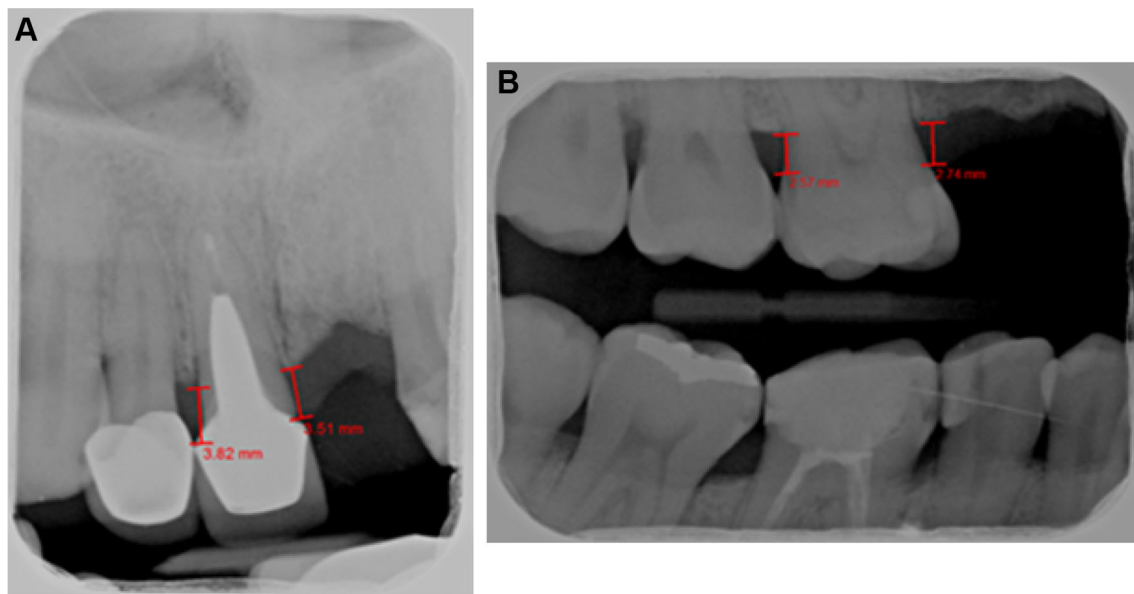


Fig. 2 Cementum–enamel junction (CEJ)–crest measurements on intraoral radiographs. **a** CEJ–crest measurements on the mesial and distal sides of a right maxillary central incisor on a periapical

radiograph. **b** CEJ–crest measurements on the mesial and distal sides of a right maxillary first molar on a bitewing radiograph

For sagittal view measurement, the plane was selected at the mesial or distal interproximal surface of the central incisor or canine, and the CEJ–crest distance was measured on both the buccal and palatal/lingual sides and then averaged (Fig. 4a). For molars, the scan was rotated to make the sagittal slice parallel with the long axis of the teeth. The CEJ–crest distance was measured on the mesial and distal sites of the buccal and lingual/palatal surfaces and then averaged (Fig. 4b).

Statistical analysis

A normal distribution of data was determined by skewness analysis and data frequency plots. One-way ANOVA followed by Tukey's HSD post hoc test was used to determine the statistical significance of differences among CAL, PA/BW, and CBCT measurements. Spearman's correlation analysis and Steiger's *Z* test were used to determine the correlations between the three evaluation methods and to detect whether there were significant differences in the correlation coefficients, respectively. The level of statistical difference was set at $p < 0.05$. All of the statistical analyses were performed with the SPSS program version 20 (IBM, Armonk, NY, USA).

Results

The periodontal measurements for central incisors, canines, and first molars of the right maxilla and left mandible were averaged for each tooth type. A normal distribution of the

data was observed at all sites with each assessment (skewness, <2) and confirmed by data frequency distribution plots (Fig. 5).

The CEJ–crest distances measured on CBCT cross-sectional views for central incisors, canines, and first molars were 2.42 ± 0.12 , 2.41 ± 0.11 , and 2.84 ± 0.16 mm, respectively. The corresponding measurements on CBCT sagittal views were 2.37 ± 0.14 , 2.39 ± 0.19 , and 2.78 ± 0.18 mm, respectively. There was no significant difference in the CEJ–crest distances measured on CBCT cross-sectional views versus sagittal views ($p > 0.05$). For simplicity, the CBCT measurements derived from cross-sectional views were used for comparisons with periodontal probing and intraoral radiographic values.

For central incisors, the CEJ–crest distances measured on CBCT and PA/BW were significantly larger than the CAL values for both mesial and distal sites (Fig. 6). For canines, CBCT demonstrated significantly larger CEJ–crest measurements compared with PA/BW and CAL (Fig. 7). For the first molars, both CBCT and CAL had significantly larger measurements than PA/BW (Fig. 8).

At all of the measured sites, Spearman's correlation analysis revealed highly significant positive correlations between CBCT and CAL, CBCT and PA/BW, and CAL and PA/BW (Fig. 9). The Pearson correlation coefficient was higher for CBCT with CAL (range $r = 0.53$ – 0.83 ; mean $r = 0.64$) relative to PA/BW with CAL (range $r = 0.44$ – 0.69 ; mean $r = 0.55$), but the difference was not significant ($Z = -1.493$; $p > 0.05$).

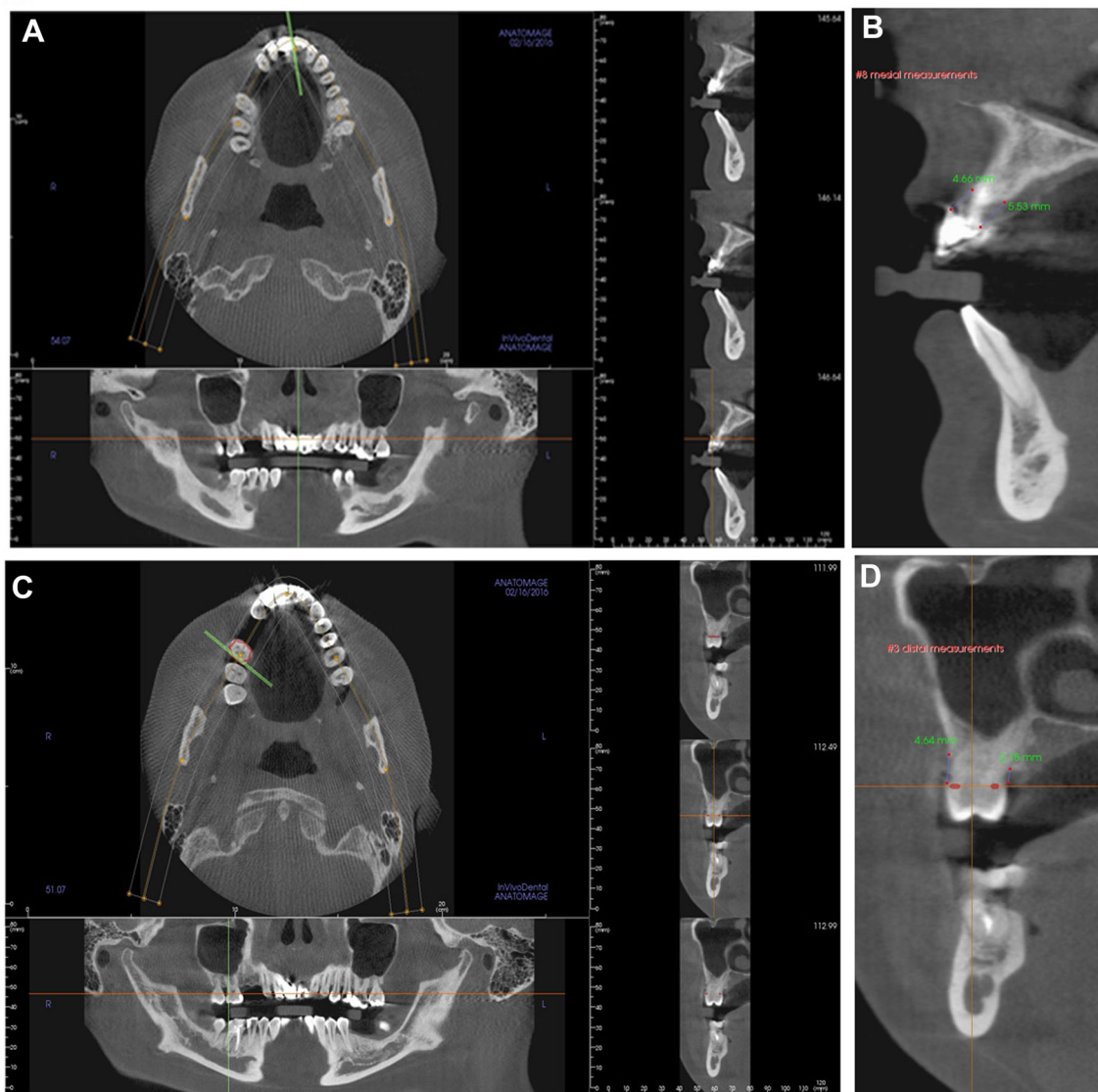


Fig. 3 Cementum–enamel junction (CEJ)–crest measurements on cone-beam computed tomography cross-sectional views. **a** Reconstructed axial, panoramic, and cross-sectional views demonstrate the selection of the cut (*green line*) along the mesial surface of a right maxillary central incisor for CEJ–crest measurements. **b** For the same tooth shown in **a**, CEJ–crest distances were measured on the buccal and palatal sides on the cross-sectional view. **c** Reconstructed axial, panoramic, and cross-sectional views demonstrate the selection of the

cut (*green line*) along the distal surface of a right maxillary first molar for CEJ–crest measurements. The nerve tracing tool was used to highlight the CEJ in *red* around the cervical area of the first molar on the axial view. **d** For the same tooth shown in **c**, the CEJ–crest distances were measured on the buccal and palatal sides on the cross-sectional view. Notice that the CEJ is shown as *red dots* at the cervical area of the molar

Discussion

In the present study, alveolar bone level was determined at the central incisor, canine, and first molar regions by CBCT and intraoral radiography, and the correlations between radiographic measurements of the alveolar bone level and the clinical attachment level were assessed. In general, CBCT generated significantly larger values than PA/BW and CAL, presumably because of the inherent differences in these imaging and evaluation methodologies. Spearman

correlation analysis revealed strong positive correlations between CBCT and PA/BW or CAL measurements, thereby establishing the validity of CBCT in periodontal assessment.

In the literature, there is no consensus regarding the direction of CBCT deviation relative to intraoral or clinical examinations. Studies have shown no difference [35, 36], underestimation [37, 38], or overestimation of CBCT measurements compared with PA/BW or periodontal probing [35, 39–41]. Many factors could potentially

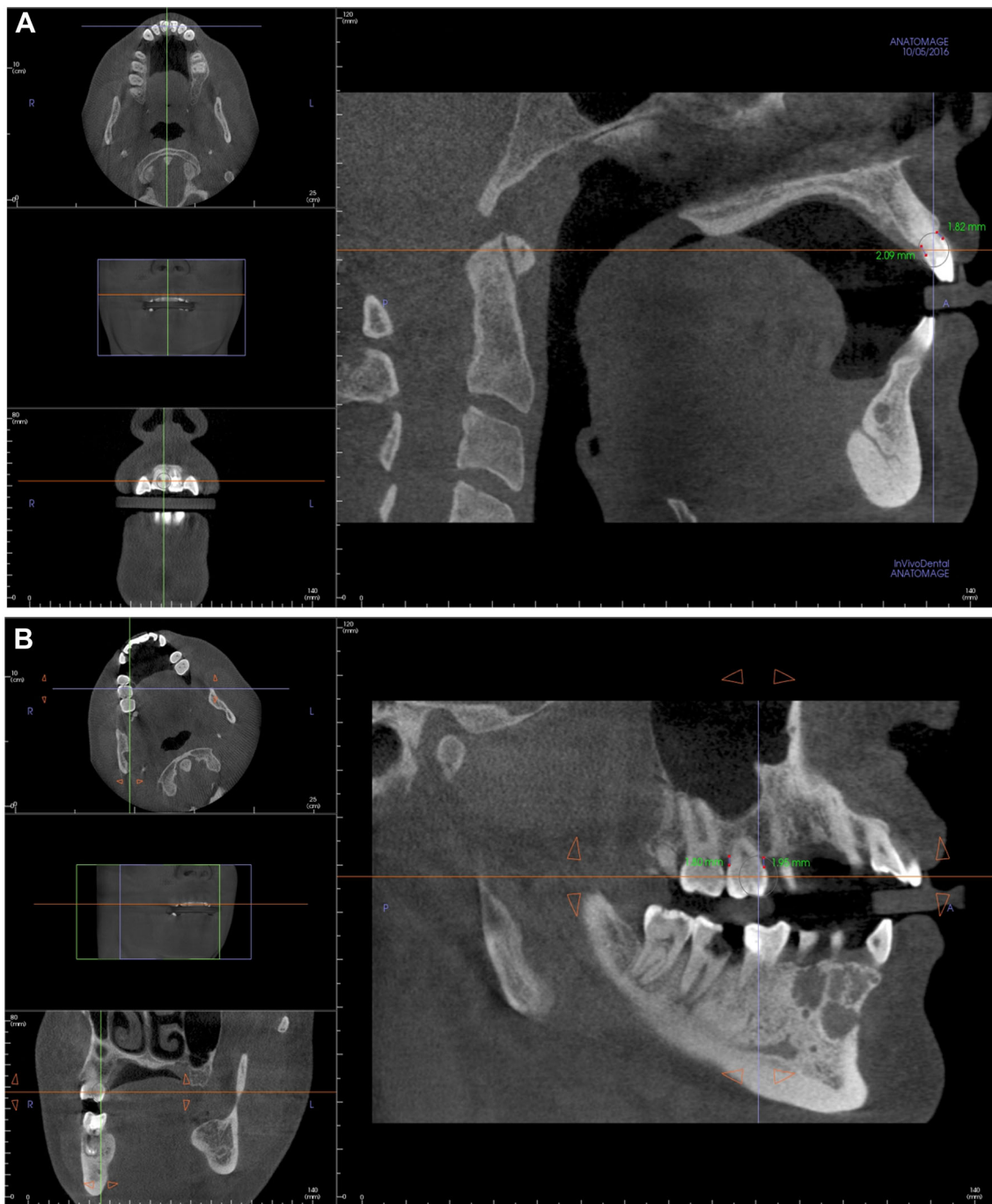


Fig. 4 Cementum–enamel junction (CEJ)–crest measurements on cone-beam computed tomography sagittal views. **a** CEJ–crest measurements on the mesial buccal and mesial palatal surfaces of a

maxillary right central incisor on the sagittal view. **b** CEJ–crest measurements on the mesial palatal and distal palatal surfaces of a maxillary right first molar on the sagittal view

contribute to these variations, such as type of CBCT unit and scanning protocol (number of slices, voxel size) [42], imaging reconstruction and measurement method (slice thickness, measurement on cross-sectional or panoramic view) [38], tooth location and surface [26, 43, 44], and training and calibration of examiners [45]. Presumably, CBCT is more accurate than PA/BW for periodontal

assessment, because it does not involve the magnification and distortion that are commonly associated with intraoral radiography. In addition, CBCT, like CAL, measures both the buccal and palatal/lingual sides of the interproximal contact areas of teeth, unlike PA/BW, which allows only one measurement with no distinctions between the buccal or palatal/lingual sides. This can probably explain why

Fig. 5 Representative plot of data showing a normal distribution. The data distribution frequencies were plotted for the right maxillary canine mesial buccal measurements on CBCT, demonstrating a normal distribution of the data set. The plots for other measurements exhibited similar patterns, indicating normal distributions of measurements at all examined tooth surfaces with all measurement strategies. *6MB* right maxillary canine mesial buccal surface, *CBCT* cone-beam computed tomography, *Std. Dev.* standard deviation

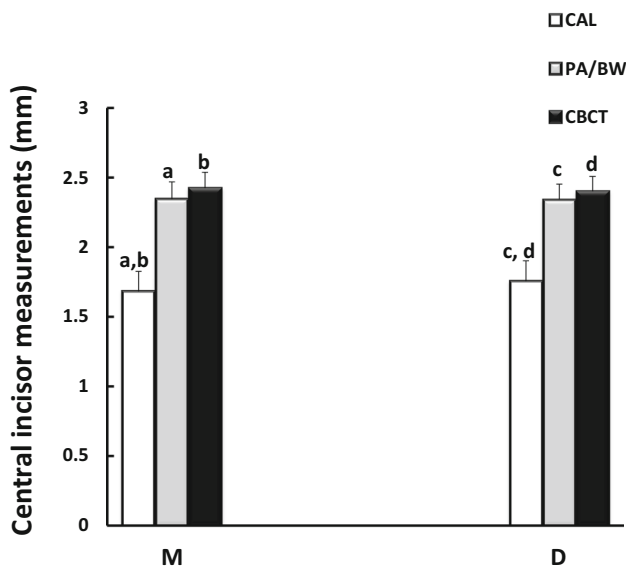
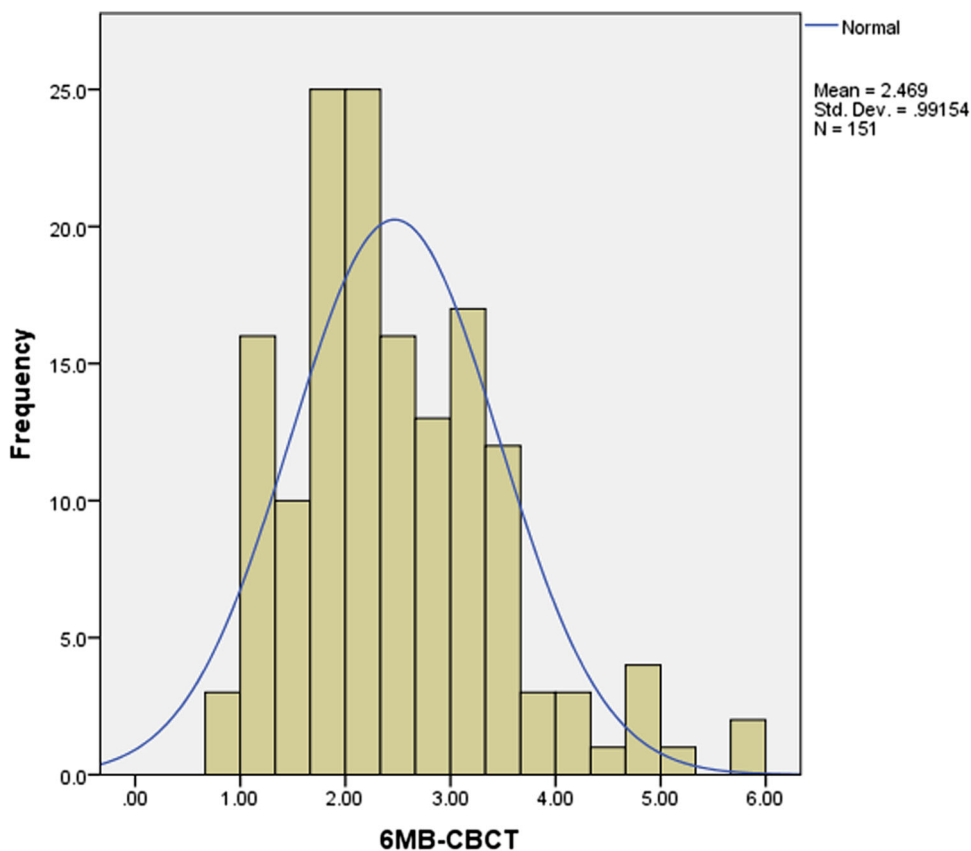


Fig. 6 Periodontal assessments of central incisors using clinical attachment level measurements, PA/BW radiographs, and CBCT images. For both the mesial and distal sides, PA and CBCT projections generated significantly larger CEJ–crest values than CAL assessments. *M* mesial, *D* distal, *CAL* clinical attachment loss, *PA/BW* periapical/bitewing radiographs, *CBCT* cone-beam computed tomography. Bars labeled with the same letter show a significant difference ($p < 0.05$)

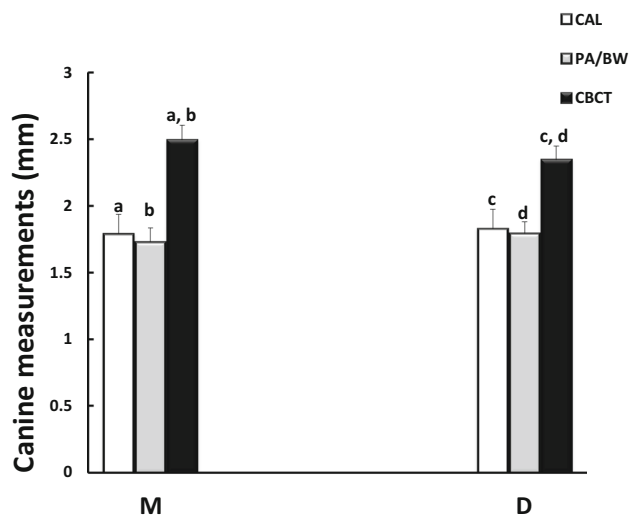


Fig. 7 Periodontal assessments of canines using clinical attachment level measurements, PA/BW radiographs, and CBCT images. For both the mesial and distal sides, CBCT projections generated significantly larger cementum–enamel junction–crest values than PA and CAL assessments. *M* mesial, *D* distal, *CAL* clinical attachment loss, *PA/BW* periapical/bitewing radiographs, *CBCT* cone-beam computed tomography. Bars labeled with the same letter show a significant difference ($p < 0.05$)

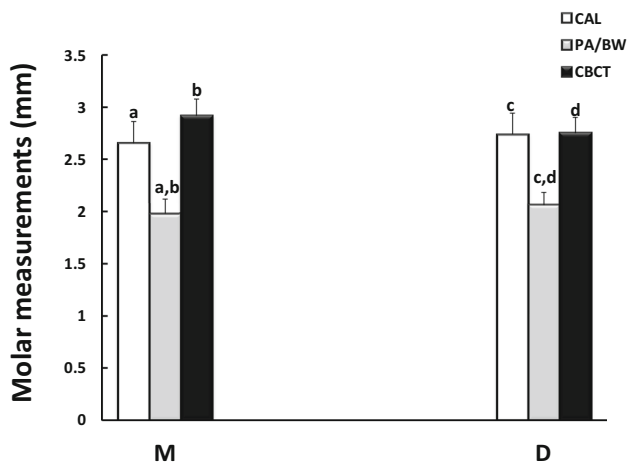


Fig. 8 Periodontal assessments of first molars using clinical attachment level measurements, PA/BW radiographs, and CBCT images. For both the mesial and distal sides, CBCT cementum–enamel junction–crest and CAL values were significantly larger than BW assessments. *M* mesial, *D* distal, *CAL* clinical attachment loss, *PA/BW* periapical/bitewing radiographs, *CBCT* cone-beam computed tomography. Bars labeled with the same letter show a significant difference ($p < 0.05$)

there was a higher (albeit not significant) correlation for CBCT with CAL, relative to that for PA/BW with CAL. However, an in-depth meta-analysis of these studies is required to reveal the underlying mechanisms for the observed inconsistency.

As a clinical investigation, the present study is among the very few *in vivo* studies that have evaluated the accuracy of CBCT in periodontal assessment. Many *in vitro* studies have used dry skulls or mandibles with no soft tissue stimulation [35, 46, 47] and radiopaque markers such as gutta percha or metallic balls to facilitate identification of the CEJ [35, 44], which are not clinically applicable. In the present study, the periodontal probing measurements, intraoral radiographs, and CBCT images were all acquired from the subjects during routine dental visits, implying their direct clinical relevance. The CEJ–crest distances were measured on both cross-sectional and sagittal CBCT views with no significant difference, indicating that either view can be suitable for periodontal assessment. In situations when the CEJ was not clearly visible on the cross-sectional view, the nerve tracing tool was used to highlight the CEJ around the cervical region on the axial view to ensure precise identification of CEJ and accurate measurement on the cross-sectional view.

The present study found a variable relationship between PA/BW and CAL assessments. At the incisor region, PA had much larger values than CAL, but at the molar region CAL had significantly larger values than BW. The presence/severity of periodontal inflammation and calculus as

well as interexaminer variation for periodontal probing could contribute to the observed differences. In addition, the projection geometry of intraoral radiographs could affect periodontal measurements. For BW radiographs, an ideal +7 to +10 vertical degree is recommended to preclude overlap of the cusps onto the occlusal surface [48]. This positive angulation may cause foreshortening, resulting in underestimation of periodontal bone loss on BW radiographs. For anterior PA radiographs, to accommodate the limitations of the anatomy, such as the shallow oral floor or presence of mandibular tori, a smaller than ideal vertical angulation can be applied, which could cause elongation and overestimation of periodontal bone loss on PA radiographs. Nevertheless, the small marginal difference between the PA/BW and clinical assessments confirms the suitability of intraoral radiography for periodontal evaluation.

The limitations of the study include the different examiners for CAL, the evaluation based on one CBCT unit and scanning protocol, and the lack of a true gold standard to compare various periodontal evaluation methods. Unlike an *in vitro* study, in which the CEJ–crest distance can be measured directly and used as the gold standard, direct clinical observation of the alveolar crest is not possible unless it is exposed surgically. The majority of the recruited subjects did not have indications for periodontal surgery, and thus the strategy for the present study was to compare and correlate the three periodontal examination methods. The obtained results confirm and validate intraoral and CBCT radiographic procedures as appropriate periodontal assessment tools with acceptable precision. More studies with different CBCT units and imaging protocols would help to further corroborate these observations.

In conclusion, as a 3D imaging modality, CBCT is superior to 2D radiography in providing morphological and topographical details for periodontal defects. The present study demonstrates that CBCT is a reliable tool for assessment of the periodontal bone level and has significant strong correlations with CAL (periodontal soft tissue examination) and PA/BW assessments. However, compared with 2D imaging, CBCT evaluation is more technically sensitive and time-consuming, because the selected measurement plane and angulation have a major impact on the assessment. It would be beneficial to develop a generally accepted protocol for periodontal assessment with CBCT. Considering the radiation dosage, CBCT performance needs to be justified prior to each scan. Patients with periodontal disease may be scanned with CBCT when the benefit for diagnosis and treatment planning outweighs the risk associated with the radiation exposure.

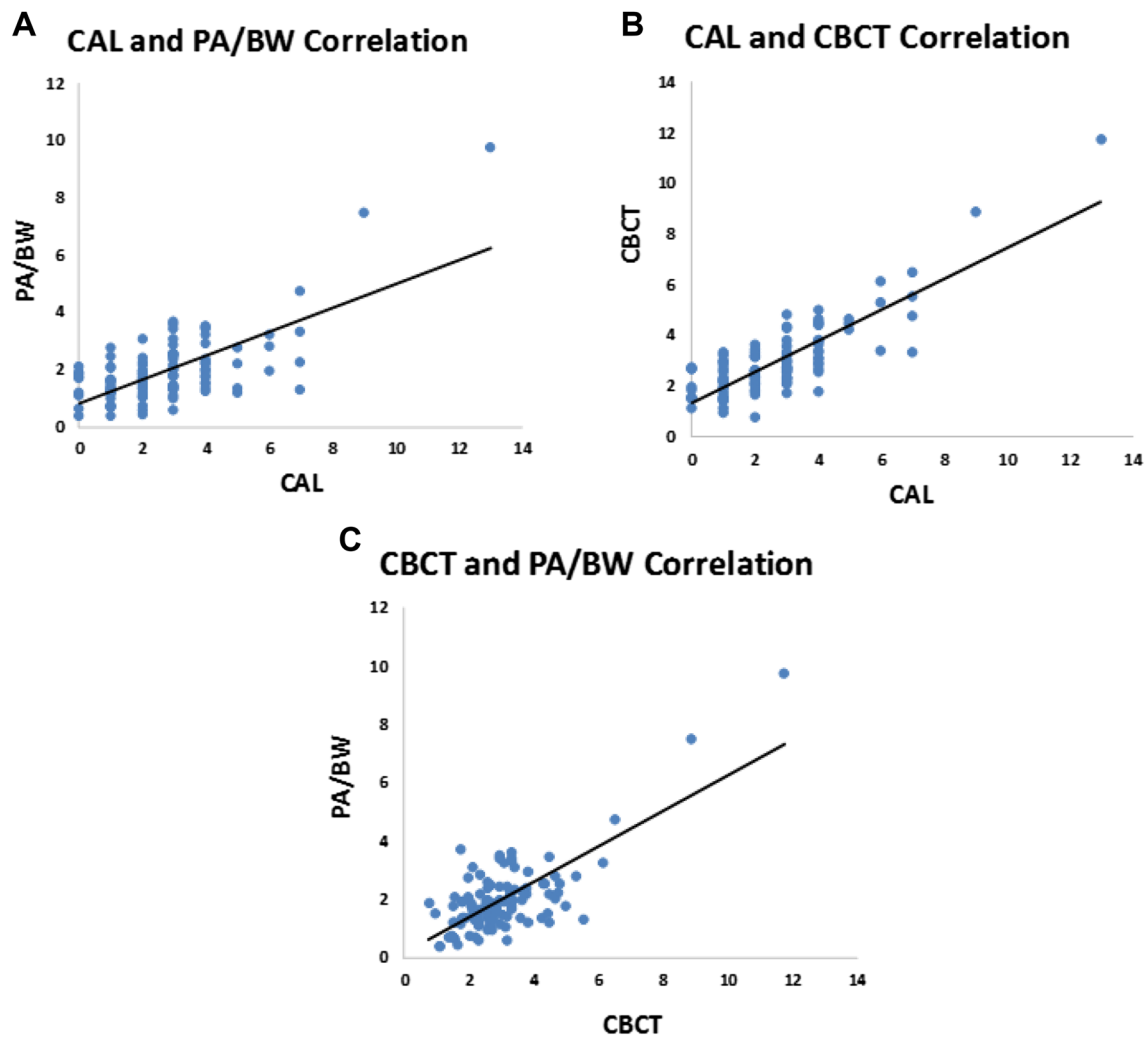


Fig. 9 Correlation analysis among clinical attachment level, PA/BW, and CBCT assessments. The illustrations represent the mesial surface of a right maxillary first molar. All other teeth and surfaces had similar correlations. **a** CAL and PA/BW assessments were highly correlated with each other. **b** CAL and CBCT assessments were

highly correlated with each other. **c** CBCT and PA/BW assessments were highly correlated with each other. CAL clinical attachment loss, PA/BW periapical/bitewing radiographs, CBCT cone-beam computed tomography

Compliance with ethical standards

Conflict of interest Wenjian Zhang, Shazia Rajani, and Bing-Yan Wang declare that they have no conflict of interest.

Human rights statement All procedures followed were in accordance with the ethical standards of the responsible national and institutional committees on human experimentation and with the Helsinki Declaration of 1964 and later versions. The Institutional Review Board (IRB) of the University of Texas Health Science Center at Houston approval was granted prior to the start of the study (HSC-DB-16-0398).

Informed consent The study was a retrospective chart review, and the requirement for informed consent was waived under IRB approval.

References

1. Loe H, Anerud A, Boysen H, Morrison E. Natural history of periodontal disease in man. Rapid, moderate and no loss of attachment in Sri Lankan laborers 14–46 years of age. *J Clin Periodontol.* 1986;13:431–45.
2. Pihlstrom BL, Michalowicz BS, Johnson NW. Periodontal diseases. *Lancet.* 2005;366:1809–20.
3. Eke PI, Dye BA, Wei L, Slade GD, Thornton-Evans GO, Borgnakke WS, et al. Update on prevalence of periodontitis in adults in the United States: NHANES 2009 to 2012. *J Periodontol.* 2015;86:611–22.
4. Eke PI, Dye BA, Wei L, Thornton-Evans GO, Genco RJ. CDC Periodontal Disease Surveillance workgroup: James Beck GDRP: prevalence of periodontitis in adults in the United States: 2009 and 2010. *J Dent Res.* 2012;91:914–20.

5. Beck JD, Eke P, Heiss G, Madianos P, Couper D, Lin D, et al. Periodontal disease and coronary heart disease: a reappraisal of the exposure. *Circulation*. 2005;112:19–24.
6. Offenbacher S. Maternal periodontal infections, prematurity, and growth restriction. *Clin Obstet Gynecol*. 2004;47:808–21.
7. Scannapieco FA. Periodontal inflammation: from gingivitis to systemic disease? *Compend Contin Educ Dent*. 2004;25:16–25.
8. Highfield J. Diagnosis and classification of periodontal disease. *Aust Dent J*. 2009;54:S11–26.
9. Holtfreter B, Alte D, Schwahn C, Desvarieux M, Kocher T. Effects of different manual periodontal probes on periodontal measurements. *J Clin Periodontol*. 2012;39:1032–41.
10. Bulthuis HM, Barendregt DS, Timmerman MF, Loos BG, van der Velden U. Probe penetration in relation to the connective tissue attachment level: influence of tine shape and probing force. *J Clin Periodontol*. 1998;25:417–23.
11. van der Velden U. Probing force and the relationship of the probe tip to the periodontal tissues. *J Clin Periodontol*. 1979;6:106–14.
12. Clerehugh V, Abdeia R, Hull PS. The effect of subgingival calculus on the validity of clinical probing measurements. *J Dent*. 1996;24:329–33.
13. Corraini P, Baelum V, Lopez R. Reliability of direct and indirect clinical attachment level measurements. *J Clin Periodontol*. 2013;40:896–905.
14. Fowler C, Garrett S, Crigger M, Egelberg J. Histologic probe position in treated and untreated human periodontal tissues. *J Clin Periodontol*. 1982;9:373–85.
15. Magnusson I, Listgarten MA. Histological evaluation of probing depth following periodontal treatment. *J Clin Periodontol*. 1980;7:26–31.
16. Hill EG, Slate EH, Wiegand RE, Grossi SG, Salinas CF. Study design for calibration of clinical examiners measuring periodontal parameters. *J Periodontol*. 2006;77:1129–41.
17. Michalowicz BS, Hodges JS, Pihlstrom BL. Is change in probing depth a reliable predictor of change in clinical attachment loss? *J Am Dent Assoc*. 2013;144:171–8.
18. Corbet EF, Ho DK, Lai SM. Radiographs in periodontal disease diagnosis and management. *Aust Dent J*. 2009;54:S27–43.
19. Hausmann E, Allen K, Clerehugh V. What alveolar crest level on a bite-wing radiograph represents bone loss? *J Periodontol*. 1991;62:570–2.
20. Jeffcoat MK. Current concepts in periodontal disease testing. *J Am Dent Assoc*. 1994;125:1071–8.
21. Reddy MS. Radiographic methods in the evaluation of periodontal therapy. *J Periodontol*. 1992;63:1078–84.
22. Bragger U. Radiographic parameters: biological significance and clinical use. *Periodontology*. 2000;2005(39):73–90.
23. Kim TS, Obst C, Zehaczek S, Geenen C. Detection of bone loss with different X-ray techniques in periodontal patients. *J Periodontol*. 2008;79:1141–9.
24. Mol A. Imaging methods in periodontology. *Periodontology*. 2000;2004(34):34–48.
25. Aljehani YA. Diagnostic applications of cone-beam CT for periodontal diseases. *Int J Dent*. 2014; doi:10.1155/2014/865079.
26. Mol A, Balasundaram A. In vitro cone beam computed tomography imaging of periodontal bone. *Dentomaxillofac Radiol*. 2008;37:319–24.
27. Pinsky HM, Dyda S, Pinsky RW, Misch KA, Sarment DP. Accuracy of three-dimensional measurements using cone-beam CT. *Dentomaxillofac Radiol*. 2006;35:410–6.
28. Raichur PS, Setty SB, Thakur SL, Naikmasur VG. Comparison of radiovisiography and digital volume tomography to direct surgical measurements in the detection of infrabony defects. *J Clin Exp Dent*. 2012;4:e43–7.
29. Dutta A, Smith-Jack F, Saunders WP. Prevalence of periradicular periodontitis in a Scottish subpopulation found on CBCT images. *Int Endod J*. 2014;47:854–63.
30. Guerrero ME, Jacobs R, Loubele M, Schutyser F, Suetens P, van Steenberghe D. State-of-the-art on cone beam CT imaging for preoperative planning of implant placement. *Clin Oral Investig*. 2006;10:1–7.
31. Honda K, Arai Y, Kashima M, Takano Y, Sawada K, Ejima K, et al. Evaluation of the usefulness of the limited cone-beam CT (3DX) in the assessment of the thickness of the roof of the glenoid fossa of the temporomandibular joint. *Dentomaxillofac Radiol*. 2004;33:391–5.
32. Liu DG, Zhang WL, Zhang ZY, Wu YT, Ma XC. Localization of impacted maxillary canines and observation of adjacent incisor resorption with cone-beam computed tomography. *Oral Surg Oral Med Oral Pathol Oral Radiol Endod*. 2008;105:91–8.
33. Nakajima K, Yamaguchi T, Maki K. Surgical orthodontic treatment for a patient with advanced periodontal disease: evaluation with electromyography and 3-dimensional cone-beam computed tomography. *Am J Orthod Dentofac Orthop*. 2009;136:450–9.
34. du Bois AH, Kardachi B, Bartold PM. Is there a role for the use of volumetric cone beam computed tomography in periodontics? *Aust Dent J*. 2012;57:103–8.
35. Misch KA, Yi ES, Sarment DP. Accuracy of cone beam computed tomography for periodontal defect measurements. *J Periodontol*. 2006;77:1261–6.
36. Vandenberghe B, Jacobs R, Yang J. Diagnostic validity (or acuity) of 2D CCD versus 3D CBCT-images for assessing periodontal breakdown. *Oral Surg Oral Med Oral Pathol Oral Radiol Endod*. 2007;104:395–401.
37. Grimard BA, Hoidal MJ, Mills MP, Mellonig JT, Nummikoski PV, Mealey BL. Comparison of clinical, periapical radiograph, and cone-beam volume tomography measurement techniques for assessing bone level changes following regenerative periodontal therapy. *J Periodontol*. 2009;80:48–55.
38. Vandenberghe B, Jacobs R, Yang J. Detection of periodontal bone loss using digital intraoral and cone beam computed tomography images: an in vitro assessment of bony and/or infrabony defects. *Dentomaxillofac Radiol*. 2008;37:252–60.
39. de Vasconcelos Faria K, Evangelista KM, Rodrigues CD, Estrela C, de Sousa TO, et al. Detection of periodontal bone loss using cone beam CT and intraoral radiography. *Dentomaxillofac Radiol*. 2012;41:64–9.
40. Fuhrmann RA, Bucker A, Diedrich PR. Assessment of alveolar bone loss with high resolution computed tomography. *J Periodontol Res*. 1995;30:258–63.
41. Takeshita WM, Iwaki LCV, Da Silva MC, Tonin RH. Evaluation of diagnostic accuracy of conventional and digital periapical radiography, panoramic radiography, and cone-beam computed tomography in the assessment of alveolar bone loss. *Contemp Clin Dent*. 2014;5:318–23.
42. Anter E, Zayet MK, El-Dessouky SH. Accuracy and precision of cone beam computed tomography in periodontal defects measurement (systematic review). *J Indian Soc Period*. 2016;20:235–43.
43. Feijo CV, Lucena JG, Kurita LM, Pereira SL. Evaluation of cone beam computed tomography in the detection of horizontal periodontal bone defects: an in vivo study. *Int J Periodontics Restor Dent*. 2012;32:e162–8.
44. Ising N, Kim KB, Araujo E, Buschang P. Evaluation of dehiscences using cone beam computed tomography. *Angle Orthod*. 2012;82:122–30.
45. Guo YJ, Ge ZP, Ma RH, Hou JX, Li G. A six-site method for the evaluation of periodontal bone loss in cone-beam CT images. *Dentomaxillofac Radiol*. 2016; doi:10.1259/dmfr.20150265.

46. Ferrare N, Leite AF, Caracas HC, de Azevedo RB, de Melo NS, de Souza Figueiredo PT. Cone-beam computed tomography and microtomography for alveolar bone measurements. *Surg Radiol Anat.* 2013;35:495–502.
47. Leung CC, Palomo L, Griffith R, Hans MG. Accuracy and reliability of cone-beam computed tomography for measuring alveolar bone height and detecting bony dehiscences and fenestrations. *Am J Orthod Dentofac Orthop.* 2010;137:S109–19.
48. White SC, Pharoah MJ. *Oral radiology principles and interpretation.* 7th ed. St. Louis: Elsevier; 2014.